Journal of Environmental Chemical Engineering 5 (2017) 4795–4802

Contents lists available at ScienceDirect

Journal of Environmental Chemical Engineering

journal homepage: www.elsevier.com/locate/jece

Research paper

Preparation and characterization of a novel magnetic biosorbent functionalized with biomass of *Bacillus Subtilis*: Kinetic and isotherm studies of biosorption processes in the removal of Methylene Blue

Bilsen Tural[a,*], Erdal Ertaş[a], Barış Enez[b], Sema Agüloğlu Fincan[c], Servet Tural[a]

[a] Department of Chemistry, Faculty of Education, Dicle University, 21280, Diyarbakir, Turkey
[b] Veterinary Health Department, Vocational School of Technical Sciences, Bingöl University, 12000 Bingöl, Turkey
[c] Department of Biology, Faculty of Science, Dicle University, 21280 Diyarbakir, Turkey

ARTICLE INFO

Keywords:
Methylene blue (MB)
Magnetic biosorbent
Magnetic separation
Biomass of *Bacillus subtilis* (*B. subtilis*)
Isotherms
Biosorption kinetics

ABSTRACT

A novel magnetic biosorbent (M-BSub) was successfully prepared by the immobilization of *Bacillus subtilis* (*B. subtilis*) with nano-sized magnetic silica which was confirmed by Fourier transform infrared spectroscopy (FTIR), thermogravimetric analysis (TGA), vibrating sample magnetometry (VSM), scanning electron microscope (SEM). Optimum biosorption conditions were determined as a function of pH, contact time and initial concentration of Methylene Blue (MB). The maximum biosorption efficiency of MB was obtained at pH 6.8 and 30 °C. The uptake of dye was very fast initially, and achieved equilibrium after 3 h. The isotherm models like Langmuir, Freundlich, Dubinin–Radushkevich (D–R) were used to analyze the equilibrium data. The equilibrium data fit better to the Freundlich model compared to the Langmuir model in concentration range studied (50–300 mg/L). The maximum biosorption capacity of biosorbent reached up to 59 ± 0.6 mg g^{-1} at pH value of 6.8 and 30 °C. The kinetics data were analyzed using adsorption kinetic models like the pseudo-first order, pseudo-second order and intraparticle diffusion equation. Kinetic data showed good agreement with the pseudo-second order kinetic model. In addition, biosorbent can be easily regenerated and reused for five cycles with high biosorption capacity. This study indicated that M-BSub is a reusable biosorbent for rapid, convenient, and efficient removal of MB from contaminated aquatic systems.

1. Introduction

Bacillus subtilis (*B. subtilis*), as an industry waste, possesses high physiological activity. The structure of the bacterial cell wall is well-known and consists mainly of teichoic acid and peptidoglycan. Teichoic acid is a bacterial copolymer of glycerol phosphate or ribitol phosphate that reveals essentially phosphate and hydroxyl groups. Peptidoglycan, also known as murein, is a polymer consisting of N-acetylmuramic and N-acetylglucosamine acids that display primarily carboxylic and hydroxyl functional groups [1].

Dyes are expansively used in several industries, like textile, rubber, cosmetics, paper, leather tanning, paint, printing, pharmaceutical, food. In textile industry alone accounts for two-three of the total dye stuff production. Even presence of small amount of dyes (below 1 mg L^{-1}) in waste water are highly toxic, undesirable, visible and serious hazards to aquatic environment [2,3].

There are two main group of techniques which have been being used to manage dye process, including effluents: Biotic and abiotic techniques. Abiotic systems consist of ion exchange, membrane, precipitation, electrochemical technologies and biosorption [4–9]. Recently, researchers have been concentrate on biological procedure for wastewater treatment, some of which are in the method of commercialisation.

Biologically based biosorption and degradation systems use cost-effective biological materials (alive or dead microorganisms). The interplay between dyes and microorganisms depends upon chemical properties of entirely the reaction samples. Every dye can have affinity to different microorganism and on the other side one microorganism is able to bind or degrade more types of dyes. At present an extensive research is carried out in many laboratories to discover optimum (and as cheap as possible) microbial biosorbent and reaction circumstances to develop an optimum technological methods enabling in order to separate polluting dyes from large volumes of contaminated water [10].

Biosorbents mostly consist from tiny particles. These particles have typical properties such as mechanical weakness, small rigidity and being not dense. Generally, their effectiveness increases with a decrease

* Corresponding author.
E-mail address: bilsentural@gmail.com (B. Tural).

http://dx.doi.org/10.1016/j.jece.2017.09.019
Received 16 June 2017; Received in revised form 9 August 2017; Accepted 9 September 2017
Available online 09 September 2017

of the particle size. In spite of their benefits, such as fine particle mass transfer, relatively cheap process price, faster reachable stable state and high potential biosorbents, they frequently have a number of drawbacks. The most significant take in solid-liquid separation problems likely biosorbent swelling and incapability to regenerate/reuse [11,12]. Solid-liquid separation is more difficult as the particle size decreases. There are several established traditional techniques which can be used for getting biosorbents proper for some applications of process. Immobilization methods like cross-linking, entrapment and covalent attachment have been found to be useful for preparation of the biosorbent [11–13]. However, efforts are still required to carry out investigation for new separation techniques.

Magnetic biosorbents can be influentially used for the separation of several types of compounds from both suspensions and solutions [11,14,15]. Magnetic field assisted separation has a number of advantages in comparison with usual separation methods. Magnetic field assisted separation method can often be applied directly in raw samples including suspended solid material. Because of the magnetic properties, magnetic biomass can be relatively, simply and selectively separated from the sample. The efficiency and power of the magnetic separation processes is useful for not only small, but also large scale operations.

Covalent attacment of biomass to magnetic nanoparticles (MNPs) is the efficient method for increasing the stability and reusability of the biosorbent [16]. In this study, we goal to synthesize M-BSub biosorbent by substitution reaction to ensure covalent attachment of *B. subtilis to* the bromopropyl-functionalized MNPs (MNP-Br). M-BSub was investigated as biosorbent to check the probability of biosorption for removing MB in aqueous solution using magnetic field assisted separation technique. Experiments are conducted so as to research the effect of diverse biosorption parameters like biosorbent dosage, the initial solution pH, and initial concentration of MB on MB removal. In order to reveal underlying mechanism about the biosorption process, some kinetic and isotherm models were assessed. Furthermore, regeneration and reuse studies of biosorbent were also carried out to determine its great significance in a more economic manner [1].

2. Materials and methods

2.1. Materials

Methylene blue ($C_{16}H_{18}ClN_3S$; MW:319.85 g mol^{-1} and λ_{max}: 663 nm) (MB), sodium hydroxide (NaOH), ammonium hydroxide (26% NH_3 in water), hydrochloric acid (37%), 3-bromopropyl-trimethoxysilane (BPTS), $FeCl_2{\cdot}4H_2O$ and $FeCl_3{\cdot}6H_2O$ were purchased from Sigma-Aldrich and all of them were of analytical grade. Different solutions at various concentrations used in different experiments were gained by dilution of the stock solution. Every reagent that used were of analytic grade and used as such.

2.2. B. subtilis cultivation

Cultivation of *B. Subtilis*, which was isolated from soil (Diyarbakır-TURKEY), was conducted in 500-mL erlenmeyer flasks including 150 mL growth media by using Nutrient Broth (NB) at pH 7.0 shaking at 150 r/min with a continuous temperature of 37 °C for 24 h. The cultures were harvested by using centrifuge (10.000 rpm,10 min). The resulting supernatants was removed and then the pellets were washed several times with 0.9% NaCl until the biomass observed whitish and the biomass dried (80 °C, 24 h). In order to obtain biomass dried cells, they were crushed in a porcelain mortar, then were autoclaved (121 °C,15 min) so as to evaluate whole death of the dried cells.

2.3. Synthesis of M-BSub

Details for synthesis and characterization of MNPs were described in our previous works [16]. The functionalization of MNPs with dead *B. subtilis* via direct coupling was carry out in two steps. In the first step, MNPs were functionalized with propyl bromide (MNP-Br). In the subsequent step, the obtained MNP-Br was reacted with *B. Subtilis*. MNP-Br was prepared following a procedure reported accordin to Zeng et al. [17]. In a typical way 1 mL (5 mmol) of (3-bromopropyl)-trimethoxysilane (BPTS) was dissolved in dry toluene (100 mL). The solution was added 1 g of MNPs and the mixture was incubated under shaking condition at 60 °C and for 18 h. The bromopropyl-functionalized MNPs (MNP-Br) was washed with toluene several times, then separated by using a magnet, finally dried by vacuum freeze dryer [18].

The substitution reaction between dead *B. subtilis* and MNP-Br for covalent immobilization of *B. subtilis* was performed as follows: 500 mg of dry and dead *B. subtilis* powder was mixed with 500 mg of MNP-Br. The mixture was wetted by adding 5 mL of distilled sterile water and thoroughly mixed. The amount of *B. subtilis* attached the MNP-Br was controlled by calculating the increase in the weight of the biomass/biosorbent after mixing the paste which was heated for 1 h oven at nearly 100 °C in order to dry the mixture. The drying and wetting steps were repeated to maximize the interaction between dead *B. subtilis* and MNP-Br, thus increasing the immobilization efficiency. The biosorbent is named as M-BSub.

2.4. Characterizations

The surface morphological features of M-BSub was analysed with scanning electron microscopy (SEM, QUANTA 200 FEG, operating at 25 kV). The magnetization values of biosorbent was studied by using vibrating sample magnetometer (VSM) at the maximum external magnetic field of 1.2 T at room temperature °C.

Fourier transformed infrared (FT-IR) spectra was measured on an Attenuated total reflectance Fourier transform infrared spectroscopy (ATR-FTIR) spectroscopy, Perkin-Elmer spectrum 100 spectrometer. Sixteen scans were collected at a resolution of 16 cm^{-1} and in the range 4000–450 cm^{-1}.

The thermal characteristic of M-BSub was measured via Thermogravimetric analysis (TGA), by using a Shimadzu DTG-60 (Japan) equipment which has properties such 10 °C/min heating rate in N_2 atmosphere. The size distribution and volume-average diameter of magnetic biosorbents were analysed by using Dynamic Light Scattering (DLS) technique (Zeta Sizer Nano-ZS, Malvern, UK).

2.5. Biosorption of MB

The biosorption of MB on the obtained M-BSub was conducted in a batch system. In the present work several effects on the biosorption of MB were studied, like the initial concentrations, the initial pH, kinetic and equilibrium parameters and the contact time. 25 mg of the biosorbent was added into 10 mL of MB solutions of desired initial concentrations (10–100 mg L-1) with a shaking of 200 rpm. The effect of pH was studied by performing series of experiments at a pH ranging from 2.0 to 10.0 with a contact time of 3 h. A solution of HCl (0.1 M) and NaOH (0.1 M) was used to adjust the pH of the solution with a shaking of 200 rpm for 3 h at 30 °C. The kinetic study of the biosorption of MB was carried out in glass bottles containing 100 mL MB by a concentration of 100 mg/L mixed with 25 mg of biosorbent. At predetermined time intervals, the samples were separated from the solution by magnetic separation and then aliquots were analyzed by measuring the absorbance using Varian Cary 100 UV/Visible Spectrophotometer in order to determine the variation of the MB concentration. The amount of MB biosorbed onto per unit mass of the biosorbent was assessed using the mass equilibrium equation:

$$q = \frac{(C_0 - C_e)V}{m} \quad (1)$$

where q (mg g^{-1}) represents the amount of biosorbed per gram of biosorbent, Ce is the equilibrium concentration and Co is the initial

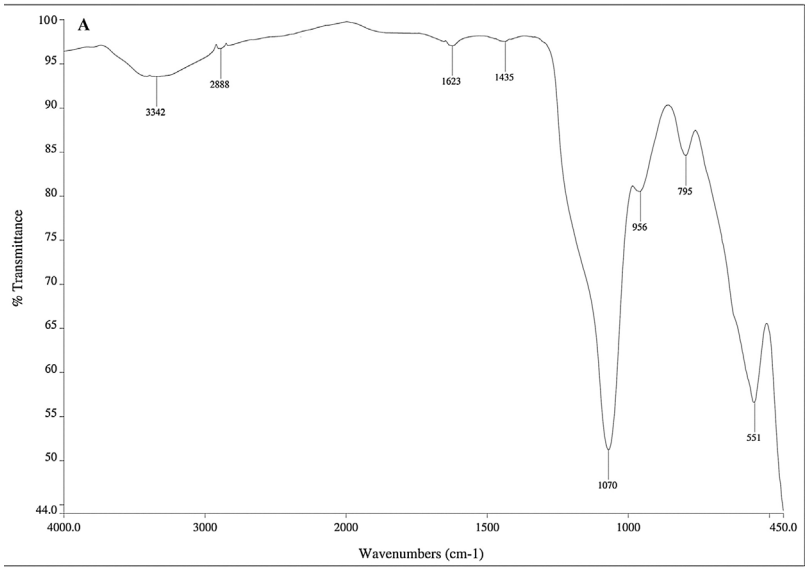

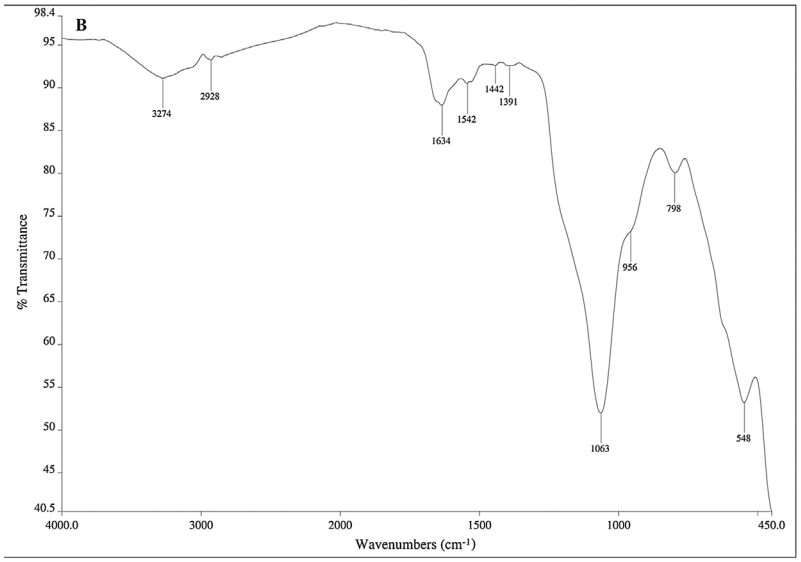

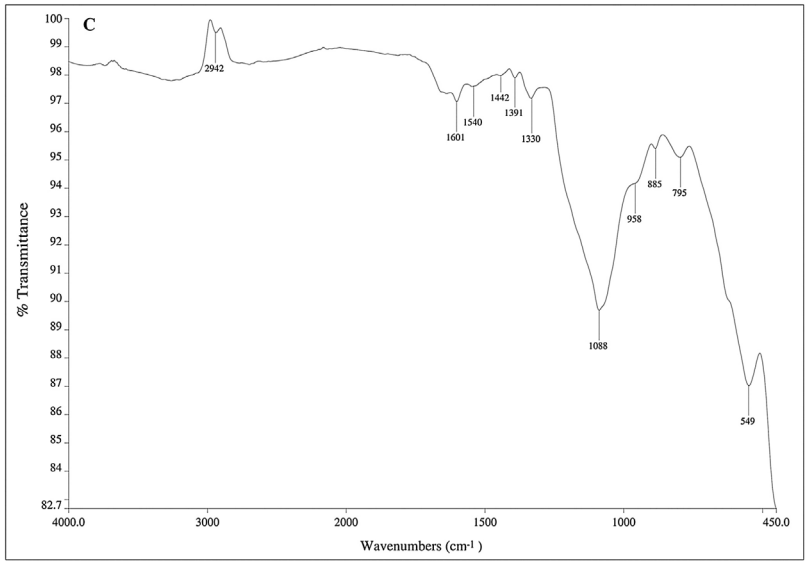

Fig. 1. FT-IR of A) MNP-Br B) M-BSub C) MB biosorbed M-BSub.

concentration of MB in aqueous solution (mg L^{-1}), V (L) is the volume of the MB solution, and m is the mass of M-BSub used (g) [19].

2.6. Desorption experiments

For the desorption experiments, 100 mg of M-BSub was inserted into 25 mL of MB aqueous solution (150 mg L^{-1}) with a shaking of 200 rpm for 3 h at 30 °C. After that, the dye loaded M-BSub were gathered and eliminated from the solution by using magnet. Then the dye loaded M-BSub was stirred with HCl solution (5 mL, pH 3.0) during 30 min period at 30 °C. The biosorbent was collected by a magnet and reused for biosorption again. The supernatant solutions were analysed by measuring the absorbance. The cycles of biosorption–desorption processes were successively conducted five times.

3. Results and discussion

3.1. Characterization of the magnetic B. subtilis

Fig. 1 shows FTIR spectra for MNP-Br, M-BSub and MB biosorbed M-BSub. *B. subtilis* is a Gram (+) microorganism. The cell walls consist from large molecules (peptidoglycan), which interrelated with polysaccharides and teichoic acid. There are several types of functional groups which belong to these molecules are carboxylate anions (–COO^-), (–NH), hydroxy (–OH), (−C═O), (–C–N–), (–C−O), (–C−H), and others. Each of them presents different affinity and can adsorb different molecules. The FTIR spectrum of MNP-Br, M-BSub and MB biosorbed M-BSub (Fig. 1 (A, B, C)) presented peaks related to the Si−O−Si bond around 1070 cm^{-1} and 795 cm^{-1}, besides a peak around 550 cm^{-1} associated with Fe-O bonds. The shoulder at approximately 950 cm^{-1} indicates the presence of Si−O−H stretching and Fe−O vibrations [20]. The band frequency around 3300 cm^{-1} indicates the hydroxyl groups exist. The band 2891, 2928 and 2938 cm^{-1} are assigned to stretching vibrations of the C−H groups. The band 1624, 1635, 1601 cm^{-1} and 1434, 1442, 1400 cm^{-1} are assigned to C−H bending vibrations of the C−H groups. In the region between 2850 and 2950 cm^{-1}, the peaks observed indicates the C−H stretching bands. The FT-IR spectrum of M-BSub (Fig. 1B) obtained from the reaction of MNP-Br with *B. subtilis* shows new peaks at 1540 and 1391 cm^{-1} related to the C═O and $-COO^-$ groups [21,22]. After biosorption of MB onto M-BSub (Fig. 1C), the characteristic peak of the C-S group in MB was observed at 1334 cm^{-1} [23,24]. Also the FT-IR spectrum of MB biosorbed M-BSub shows a new peak at 885 cm^{-1}, which is due to the hydrogen bonds formation between the heterocyclic N atoms of MB and H atoms of M-BSub. It is suggesting that the process of MB biosorption on the M-BSub was mainly a physical biosorption [24].

In order to reveal the content of organic functional groups of biosorbent, thermogravimetric (TGA) methods were also used (Fig. 2a). For the case of MNP-Br, it seems as such; under 200 °C weight loss generally caused by loss of water desorption from its surface; while it seems to be caused from release of water over 600 °C. As it is revealed from the TGA curve of M-BSub, a weight loss (21 wt.%) between 200 and 600 °C, caused by decomposition of *B. Subtilis* which is inserted in the surface of MNP-Br, except water loss events [25].

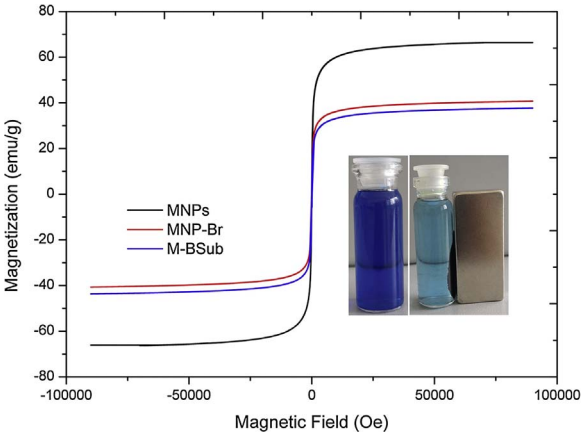

Fig. 3. Room-temperature magnetization curves for the MNPs, MNP-Br and M-BSub.

The distribution and size of particles/agglomerates of the MNPs, MNP-Br and M-BSub are demonstrated in Fig. 2b. The average particle size (z-average) of the MNPs, MNP-Br and M-BSub were decided as 165 nm, 955 nm and 1096 nm, respectively. As can be seen from Fig. 2b, the size of MNPs increased from 165 to 955 nm when they were coated with BPTS. The particle size of the MNP-Br and M-BSub were compared with each other. The particle size of the MNP-Br was increased from 955 to 1096 nm when they were successfully functionalized with *B. Subtilis* (Fig. 2b).

Magnetic property measurement indicates that MNPs, MNP-Br and M-BSub have saturation magnetization values of 66.4, 40.7 and 37.7 emu/g, respectively (Fig. 3). These results showed that the magnetization of MNPs decreased substantially with the increase of BPTS and *B.Subtilis* organic groups. As can be seen from the inset in Fig. 3 shows, the MB dye biosorbed M-BSub was highly responsive to a magnetic field, where the suspension was clarified in 20 s by using a permanent magnet [26].

The morphology and structure of the M-BSub and MB sorbed M-BSub were characterized by SEM [26]. M-BSub and MB sorbed M-BSub show spherical in shape and particulate structure with a fairly uniform size distribution. SEM indicated slight differences in the morphology of M-BSub and MB biosorbed M-BSub biosorbent (Fig. 4). Unlike MB biosorbed M-BSub, the surface of M-BSub is relatively smooth (Fig. 4a).

3.2. Effect of various parameters onto the biosorption of MB

3.2.1. The effect of pH

The pH of the solution is one of the major factors influencing biosorption of dyes. The impact of the pH value of initial solution to the biosorption of MB onto M-BSub was studied between pH 2.0 and pH 10.0 at 298 K for 3 h. The initial value of concentration belongs to MB was 100 mgL^{-1}. Fig. 5a shows the impact of pH on the MB removal effectiveness onto the M-BSub.

Methylene Blue is a heterocyclic aromatic compound having the

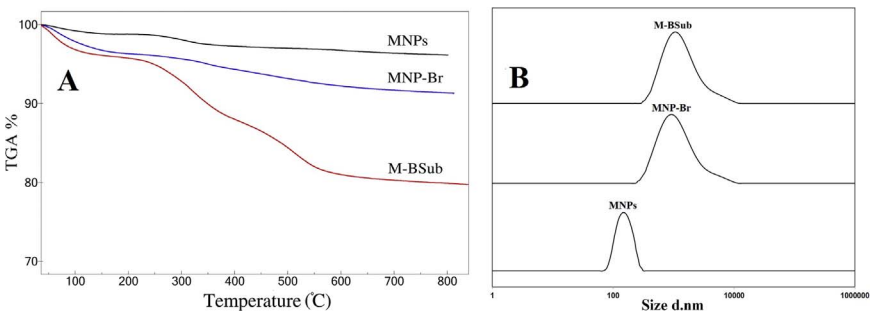

Fig. 2. Characterization of MNPs, MNP-Br and M-BSub A) TGA curves; B) Particle size distribution.

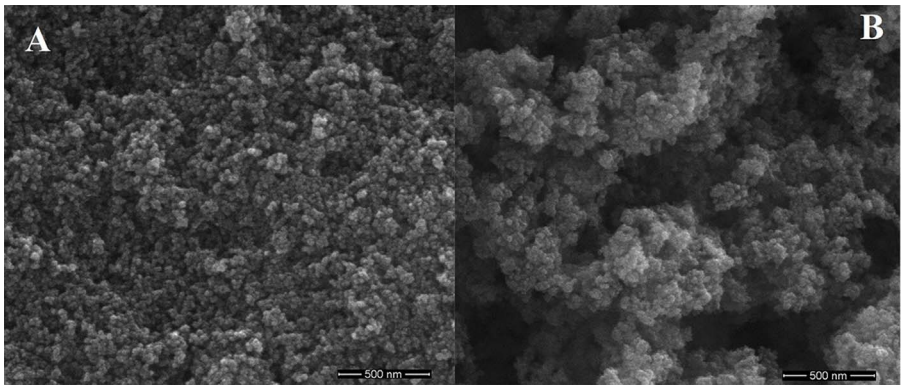

Fig. 4. A) SEM graphs of the M-BSub and B) MB biosorbed M-BSub.

chemical formula $C_{16}H_{18}N_3SCl$. The MB dye generally classified as a very weak basic dye and cationic kinds because of the presence of positively charge quaternary nitrogen atoms [27].

In this case, in the acidic pH conditions, positively charged surface sites on M-BSub did not support the biosorption of dye cations because of the electrostatic repulsion. Furthermore, lower biosorption of MB at under pH 6.8 might also be caused from competitional interaction between the cationic methylene blue dye and excess hydronium ions (H^+) at active biosorption sites. Nevertheless, in spite of the electrostatic thrust and/or hydronium ions (H^+) competition, a significant amount of MB was biosorbed by M-BSub at acidic pH values (Fig. 5a), which proposed that other mechanisms might involve in the MB biosorption process. It was considered that the OH^- group of M-BSub could bind with the =N of the MB molecule via hydrogen (H−) bonding which also contributed toward biosorption of MB molecules onto M-BSub [28]. Furthermore, the nitrogen atom of MB might interact with groups of M-BSub through lewis acid-base interaction, since the MB has acted as a lewis base. On the other hand, under alkaline conditions, MB tends to form cations, whereas OH^- is biosorbed to the surface of M-BSub to form negatively charged biosorption centres, thereby promoting the biosorption of MB ions [29]. The effect of pH was studied by performing series of experiments at a pH ranging from 2.0 to 10.0 with a contact time of 3 h and the best outcome was obtained at pH 6.8. A decrease of loading capacity was seen after pH 6.8 while we expected to see an increase of the attaching capacity. The reason is probably the decomposition of the coating material [30,31].

3.2.2. The effect of contact time

The biosorption kinetics of MB are shown in (Fig. 5b). It was observed that the MB uptake capacities increased with time and reached equilibrium values at about 180 min [32,33]. After that MB uptake became much less significant. It was likely owing to the initial large quantity of the active sites of M-BSub at the beginning of the biosorption process and as time increases and these sites gradually captured, the biosorption is becoming less efficient [34]. In the following experiments, 180 min is selected to achieve the biosorption equilibrium.

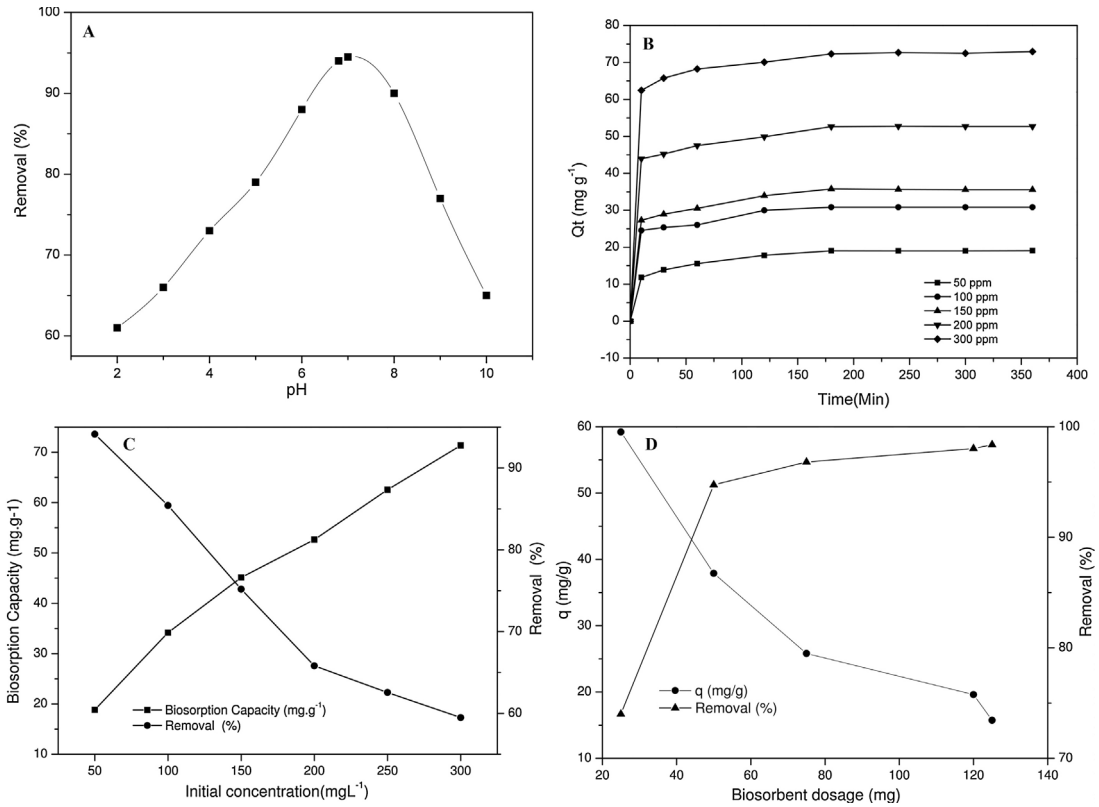

Fig. 5. A) The effect of pH on biosorption B) The effect of time MB concentrations on biosorption C) The effect of initial MB concentrations on the biosorption capacity and dye removal percentages D) The effect of M-BSub dosage on the biosorption capacity and dye removal percentages.

3.2.3. The effect of initial concentration of MB

The effect of initial concentration of MB on percentage removal efficiency and biosorption capacity is shown in (Fig. 5c). The biosorption experiments were conducted at 30 °C by mixing 25 mg of M-BSub at different concentrations of the MB (ranging from 50 mg L^{-1} to 300 mg L^{-1}) at pH 6.8 for 3 h. It was observed that 94% of MB was removed with 50 mg/L initial concentration, then reduces with the increase of initial MB concentration. The high biosorption effectiveness (close to 95%) at low concentrations indicates the practical application of M-BSub for removal of trace amount of MB from wastewater. The removal efficiency of MB drops harshly (60%) with an increase at initial concentration of MB from 50 to 300 mg/L. This is due to the fact that the saturation of binding sites at high concentrations leads to more MB ions unsorbed in solution [35]. However, the biosorption capacity of M-BSub grows up with increasing initial MB concentration, and reaches 72 mg/g with 300 mg/L initial concentration of MB. This can be attributed to the fact that the higher MB concentrations increase the overall mass transfer driving force and thus the MB uptakes onto the biosorbent [1].

3.2.4. The effect of dosage

To investigate the effect of biosorbent dosages on the percentage removal and biosorption capacity of MB, was investigated by adding various amounts of the M-BSub to MB solutions followed by shaking at room temperature for 3 h at 30 °C (Fig. 5d). It is clearly seen that the removal efficiency of MB dye increased with increasing M-BSub dosage, which was because of more biosorption sites being available at higher biosorbent dosages. However, when the biosorption reaches a saturated state, no more MB dye can be biosorbed onto the biosorbent even if the dosage of the biosorbent is increased. The results indicated that the removal efficiency reached an equilibrium at 98% for MB, corresponding to 25 mg M-BSub biosorbent dosage. However, a decrease in the value of q was observed from 59 mg/g to 16 mg/g, for MB. The decrease in the amount of dye biosorbed per gram of the biosorbent with increase in the biosorbent dose is mainly due to instauration of biosorption sites through the biosorption process. Considering the removal efficiency and practicality, the optimum biosorbent dosage was maintained at 25 mg for MB in all subsequent experiments.

3.3. Biosorption isotherm studies

The equilibrium biosorption isotherm is significant in explaining the interactive behavior between solutes and biosorbent and is main in the design of biosorption system. Three models usually used to simulate the biosorption isotherm are the Langmuir, Freundlich and Dubinin–Radushkevich (D–R) isotherms [36,37].

Langmuir isotherm [38] is a model for monolayer localized physical biosorption on homogeneous surface. It is based on the three hypotheses: monolayer coverage, uniformly energetic biosorption sites, and without any lateral interaction between biosorbed molecules. The Langmuir isotherm equation has a hyperbolic form.

$$q_e = \frac{q_{\max} K_L C_e}{1 + K_L C_e} \tag{2}$$

The Langmuir isotherm model can be decided to following linearized form;

$$\frac{1}{q_e} = \frac{1}{q_{\max}} + \left(\frac{1}{q_{\max} K_L}\right)\frac{1}{C_e} \tag{3}$$

where q_{max} the maximum biosorption capacity of the biosorbent for MB ions (mg g^{-1}); q_e is the amount biosorbed at equilibrium (mg g^{-1}); K_L is the biosorption intensity related to the affinity of the linking site and Ce the equilibrium concentration of the MB ions (mg L^{-1}). The linear plots of 1/Ce vs 1/qe show that biosorption follows the Langmuir biosorption isotherm model.

Dimensionless quantity biosorption parameter R_L, equilibrium parameter (also called as separation factor) represents properties of Langmuir isotherm [39,40] and is defined as:

$$R_L = \frac{1}{1 + K_L C_o} \tag{4}$$

where, C_0 is highest concentration of MB in the solution (mg L^{-1}) and K_L (Lmg^{-1}) is maximum biosorption capacity. The experimental data R_L values lie between 0 and 1, which indicates favorable biosorption of MB onto M-BSub [41,42]. The value of R_L in the present study was found 0.021, hence, biosorption of MB was favorable.

The Freundlich isotherm can be used as an empirical equation the biosorption intensity of the biosorbent towards the biosorbate and is expressed as [43].

$$q_e = K_F C_e^{1/n} \tag{5}$$

It is convenient to use the well-known logarithmic form of Freundlich isotherm in the linear form, which can be easily obtained by taking logarithm of equation;

$$\ln q_e = \ln K_F + \frac{1}{n} \ln C_e \tag{6}$$

where K_F is the Freundlich constant associated with biosorption capacity of biosorbent, n is the Freundlich constant related with biosorption dimensionless (intensity).

The D–R isotherm equation is used in order to determine the nature of MB biosorption by the biosorbent as chemical or physical. The D–R equation [44] is:

$$q_e = {}^{g_{\max} e^{-\beta\varepsilon^2}} \tag{7}$$

The linearized form of (D-R) equation is represented as follows;

$$\ln q_e = \ln q_{\max} - \beta\varepsilon^2 \tag{8}$$

where β is the D-R constant related with the mean free energy of biosorption (mol^2/J^2), qe is the amount of biosorbate per unit weight of biosorbent (mol/g), ε is the Polanyi potential and q_{max} is the maximum biosorption capacity (mg/g). E (kJ/mol) is the mean biosorption energy that is obtained from equation (8) [45]:

$$E = \frac{1}{\sqrt{(2\beta)}} \tag{9}$$

The E values state the type of biosorption process. It is known that if E is physical and chemical biosorptions occurred when $E < 8$ and $E > 16$ kJ/mol, respectively. In this work, E value determined from the D-R model is 0.500 kJ/mol, showing that the biosorption of MB onto M-BSub is mainly physical adsorption. Table 1 shows the results of Freundlich, Langmuir and D–R isotherm parameters. It is revealed that all of the isotherms proper very well when the R^2 values are related.

3.4. Kinetic studies

In this paper, the intraparticle diffusion, pseudo-first-order and

Table 1
Biosorption isotherm parameters for MB.

Isotherm models	Parameters	Value
Langmuir	q_{max} (mg g^{-1})	59 ± 0.6
	K_L (L/mg)	0.158
	R_L	0.021
	R^2	0.953
Freundlich	K_F (mg/g)	13.37
	n	2.98
	R^2	0.994
Dubinin-Radushkevich	B (mol^2/kJ^2)	2×10^{-6}
	q_{max} (mg g^{-1})	53 ± 1.3
	E (mol^2/kJ^2)	500
	R^2	0.754

Table 2
Kinetic parameters for biosorption of MB onto M-BSub.

Kinetic model	Parameter	50 ppm	100 ppm	150 ppm	200 ppm	300 ppm
Pseudo-first-order	k_1 (mg min g^{-1})	0.020	0.024	0.019	0.018	0.022
	q_e (mg g^{-1})	11.87	15.4	17.32	19.55	22.62
	R^2	0.906	0.832	0.799	0.657	0.669
Pseudo-second-order	k_2 (mg min g^{-1})	0.013	0.008	0.006	0.002	0.001
	q_e (mg g^{-1})	19.49	31.54	36.10	53.19	73.52
	R^2	0.998	0.999	0.999	0.999	0.999
Intraparticle diffusion	Kp(mgg^{-1} $min^{-1/2}$)	0.461	0.459	0.570	1.869	2.475
	C	11.56	23.35	26.31	24.91	36.42
	R^2	0.879	0.869	0.890	0.532	0.484

pseudo-second order equations were used in order to examine kinetic properties of MB dye onto M-BSub [46–48]. The linearized form each equation is represented as follows:

Pseudo-first order equation:

$$\ln(q_e - q_t) = \ln q_e - k_1 t \quad (10)$$

and the second-order equation:

$$\frac{t}{q_t} = \frac{1}{k_2 q_e^2} + \frac{1}{q_e} t \quad (11)$$

where q_t is the adsorption capacity of dye (mg/g) at a given time t, and q_e is the adsorption capacity of dye (mg/g) at equilibrium. Also k_1 (min^{-1}) and k_2 (g/mg min) are the first-order and the second-order rate constants, respectively.

Intraparticle diffusion equation:

$$q_t = k_p t^{0.5} + C \quad (12)$$

where C is a constant and k_p is the intraparticle diffusion rate constant (mg/g $min^{1/2}$). This equation q_t versus $t^{1/2}$ should be linearized intraparticle diffusion is consist of the biosorption process. The linear regression coefficient, R^2 and parameters of kinetics equations are catalogued in Table 2.

3.5. Reusability

The reusability of biosorbent was studied for five times as shown in Fig. 6. The reusability of the biosorbent after five consecutive uses was obtained to be 95, 85, 74, 65, 60%. These results show that the M-BSub can be manipulated as effective biosorbent for removing MB dye in waste water.

3.6. Comparison with other sorbents

Biosorption experiments were performed using M-BSub for MB removal. The biosorption capacity of MB onto M-BSub was compared

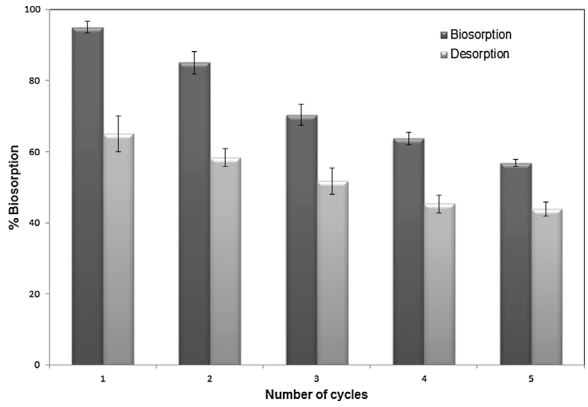

Fig. 6. Reusability of M-BSub for MB biosorption.

Table 3
Comparison of biosorption capacities of various biosorbents with M-BSub for MB removal.

Biosorbent	Biosorption capacity Q^0 (mg g^{-1})	Reference
Duckweed (Spirodela polyrrhiza) (at pH 7)	119	[49]
Unmodified biomass of baker's yeast	51.5	[50,51]
Dead Streptomyces rimosus	34.34	[52]
Dead fungusAspergillus niger	18.54	[53]
Posidonia oceanica (L.) fibres	5.56	[54]
Caulerpa racemosavar.cylindracea	5.23	[55]
Living biomass	1.17	[53]
M-BSub	59 ± 0.6	This study

with different sorbents that are reported in literature and represented in Table 3. A comparison of adsorption capacities of various biosorbents shows that M-BSub can be considered as the potential biosorbent for the removal of MB from aqueous solutions.

4. Conclusion

In this study, the *B. subtilis* linked MNPs were offered as a biosorbent for magnetic separation of MB dye and examined the equilibrium and the dynamics of the biosorption. M-BSub seemed convenient for the dye separation process, by its size and biosorption properties. The MB biosorption capacity of the M-BSub was depend on the initial dye concentration, pH, dosage of biosorbent and contact time. Solution pH played an important role on MB removal for the biosorbent examined. When initial dye concentration increased, the biosorption capacity increased also accordingly. The isotherm models like Langmuir, Freundlich, Dubinin–Radushkevich (D–R) were used to analyze the equilibrium data. The equilibrium biosorption phenomena were found to be well described by the Freundlich isotherm model rather than the Langmuir model in concentration range studied (50–300 mg/L). The maximum biosorption capacity of M-BSub reached up to 59 ± 0.6 mg g^{-1} at pH value of 6.8 and 30 °C. Kinetic studies suggest that MB biosorption described more favorably by the pseudo-second order kinetic model. Additionally, by using pH 3 acidic solution M-BSub can be efficiently regenerated, and the M-BSub can be used for the MB removal repeatedly up to five cycle. In this work, a convenient and efficient method is offered for the M-BSub biosorbent preparation, which relieved a more effective biosorption of MB from aqueous solution (sorbed 95% of MB), and also avoided the risk of extra pollution of water by M-BSub. In this study, the magnetic separation method is used. This method has some benefits such as simple sample handling, potential for study with big sample volumes, without filtration or centrifugation or decantation steps.

Acknowledgements

This project is funded by the financial support from Dicle University

Research Fund (DUBAP, 13-ZEF-28, ZGEF.16.008, ZGEF.17.008) and the Scientific and Technological Research Council of Turkey (TUBITAK, 109T497), COST Action CM0701.

References

[1] Y.-g. Liu, L. Ting, Z.-b. He, T.-t. Li, W. Hui, X.-j. Hu, Y.-m. Guo, H. Yuan, Biosorption of copper (II) from aqueous solution by Bacillus subtilis cells immobilized into chitosan beads, Trans. Nonferrous Met. Soc. China 23 (2013) 1804–1814.

[2] I.M. Banat, P. Nigam, D. Singh, R. Marchant, Microbial decolorization of textile-dyecontaining effluents: a review, Bioresour. Technol. 58 (1996) 217–227.

[3] T. Robinson, G. McMullan, R. Marchant, P. Nigam, Remediation of dyes in textile effluent: a critical review on current treatment technologies with a proposed alternative, Bioresour. Technol. 77 (2001) 247–255.

[4] J. Forss, U. Welander, Decolourization of reactive azo dyes with microorganisms growing on soft wood chips, Int. Bıodeter. Bıodegr. 63 (2009) 752–758.

[5] V. Gomez, M. Larrechi, M. Callao, Kinetic and adsorption study of acid dye removal using activated carbon, Chemosphere 69 (2007) 1151–1158.

[6] Y.S. Ho, G. McKay, Sorption of dye from aqueous solution by peat, Chem. Eng. J. 70 (1998) 115–124.

[7] T.B. Iyim, G. Güçlü, Removal of basic dyes from aqueous solutions using natural clay, Desalination 249 (2009) 1377–1379.

[8] V.S. Mane, I.D. Mall, V.C. Srivastava, Kinetic and equilibrium isotherm studies for the adsorptive removal of Brilliant Green dye from aqueous solution by rice husk ash, J. Environ. Manage. 84 (2007) 390–400.

[9] S.K. Parida, B.K. Mishra, Adsorption of styryl pyridinium dyes on silica gel, J. Colloid. Interface. Sci. 182 (1996) 473–477.

[10] I. Safarik, L. Ptackova, M. Safarikova, Adsorption of dyes on magnetically labeled baker's yeast cells, Eur. Cells. Mater. 3 (2002) 52–55.

[11] N. Saravanan, T. Kannadasan, C.A. Basha, V. Manivasagan, Biosorption of textile dye using immobilized bacterial (Pseudomonas aeruginosa) and fungal (Phanerochate chrysosporium) cells, Am. J. Environ. Sci. 9 (2013) 377–387.

[12] K. Vijayaraghavan, M.W. Lee, Y.S. Yun, A new approach to study the decolorization of complex reactive dye bath effluent by biosorption technique, Bioresour. Technol. 99 (2008) 5778–5785.

[13] B. Volesky, Detoxification of metal-bearing effluents: biosorption for the next century, Hydrometallurgy 59 (2001) 203–216.

[14] M. Šafaříková, L. Ptáčková, I. Kibrikova, I. Šafařík, Biosorption of water-soluble dyes on magnetically modified *Saccharomyces cerevisiae subsp. uvarum* cells, Chemosphere 59 (8) (2005) 831–835.

[15] Z. Saiyed, S. Telang, C. Ramchand, Application of magnetic techniques in the field of drug discovery and biomedicine, Biomagn. Res. Technol. 1 (2003) 1–2.

[16] B. Tural, S. Tural, E. Ertaş, İ. Yalınkılıç, A.S. Demir, Purification and covalent immobilization of benzaldehyde lyase with heterofunctional chelate-epoxy modified magnetic nanoparticles and its carboligation reactivity, J. Mol. Catal. B. Enzym. 95 (2013) 41–47.

[17] T. Zeng, L. Yang, R. Hudson, G. Song, A.R. Moores, C.J. Li, Fe_3O_4 nanoparticle-supported copper (I) pybox catalyst: magnetically recoverable catalyst for enantioselective direct-addition of terminal alkynes to imines, Org. Lett. 13 (2010) 442–445.

[18] A. Maleki, Z. Alrezvani, S. Maleki, Design, preparation and characterization of urea-functionalized Fe_3O_4/SiO_2 magnetic nanocatalyst and application for the one-pot multicomponent synthesis of substituted imidazole derivatives, Catal. Commun. 69 (2015) 29–33.

[19] L. Ai, C. Zhang, Z. Chen, Removal of methylene blue from aqueous solution by a solvothermal-synthesized graphene/magnetite composite, J. Hazard. Mater. 192 (2011) 1515–1524.

[20] G. Liu, H. Wu, H. Zheng, L. Tang, H. Hu, H. Yang, S. Yang, Synthesis and applications of fluorescent-magnetic-bifunctional dansylated $Fe_3O_4@SiO_2$ nanoparticles, J. Mater. Sci. 46 (2011) 5959–5968.

[21] C. Ding, W. Cheng, Y. Sun, X. Wang, Effects of *Bacillus subtilis* on the reduction of U (VI) by nano-Fe0, Geochim. Cosmochim. Acta 165 (2015) 86–107.

[22] Y. Guo, W. Du, S. Wang, L. Tan, The biosorption of Sr (II) on *Bacillus subtilis*: a combined batch and modeling study, J. Mol. Liq. 220 (2016) 762–767.

[23] A.D. Cross, An Introduction to Practical Infrared Spectroscopy, Butterworths Scientific Publications, London, 1960.

[24] O.V. Ovchinnikov, A.V. Evtukhova, T.S. Kondratenko, M.S. Smirnov, V.Y. Khokhlov, O.V. Erina, Manifestation of intermolecular interactions in FTIR spectra of methylene blue molecules, Vib. Spectrosc. 86 (2016) 181–189.

[25] Z. Lei, Y. Li, X. Wei, A facile two-step modifying process for preparation of poly (SStNa)-grafted Fe_3O_4/SiO_2 particles, J. Solid. State. Chem. 181 (2008) 480–486.

[26] M.A. Ghasemzadeh, M.H. Abdollahi-Basir, M. Babaei, $Fe_3O_4@SiO_2$-NH_2 core-shell nanocomposite as an efficient and green catalyst for the multi-component synthesis of highly substituted chromeno [2,3-b] pyridines in aqueous ethanol media, Green Chem. Lett. Rev. 8 (2015) 40–49.

[27] W. Wei, L. Yang, W. Zhong, S. Li, J. Cui, Z. Wei, Fast removal of methylene blue from aqueous solution by adsorption onto poorly crystalline hydroxyapatite nanoparticles, Digest. J. Nanomat. Biostruct. 19 (2015) 1343–1363.

[28] P. Sharma, M.R. Das, Removal of a cationic dye from aqueous solution using graphene oxide nanosheets: investigation of adsorption parameters, J. Chem. Eng. Data 58 (2012) 151–158.

[29] D. Chen, Z. Zeng, Y. Zeng, F. Zhang, M. Wang, Removal of methylene blue and mechanism on magnetic γ-Fe_2O_3/SiO_2 nanocomposite from aqueous solution, Water. Res. Ind. 15 (2016) 1–13.

[30] B. Tural, T. Tarhan, S. Tural, Covalent immobilization of benzoylformate decarboxylase from Pseudomonas putida on magnetic epoxy support and its carboligation reactivity, J. Mol. Catal. B: Enzym. 102 (2014) 188–194.

[31] B. Tural, I. Simsek, S. Tural, B. Çelebi, A.S. Demir, Carboligation reactivity of benzaldehyde lyase (BAL, EC 4.1. 2.38) covalently attached to magnetic nanoparticles, Tetrahedron: Asymmetry 24 (2013) 260–268.

[32] B. Heibati, S. Rodriguez-Couto, N.G. Turan, O. Ozgonenel, A.B. Albadarin, M. Asif, I. Tyagi, S. Agarwal, V.K. Gupta, Removal of noxious dye—acid orange 7 from aqueous solution using natural pumice and Fe-coated pumice stone, J. Ind. Eng. Chem. 31 (2015) 124–131.

[33] C.F. Chang, C.Y. Chang, K.H. Chen, W.T. Tsai, J.L. Shie, Y.H. Chen, Adsorption of naphthalene on zeolite from aqueous solution, J. Colloid. Interf. Sci. 277 (2004) 29–34.

[34] A. Saeed, M. Sharif, M. Iqbal, Application potential of grapefruit peel as dye sorbent: kinetics, equilibrium and mechanism of crystal violet adsorption, J. Hazard. Mater. 179 (2010) 564–572.

[35] C. Yang, J. Wang, M. Lei, G. Xie, G. Zeng, S. Luo, Biosorption of zinc (II) from aqueous solution by dried activated sludge, J. Environ. Sci. 22 (2010) 675–680.

[36] A.K. Hammed, N. Dewayanto, D. Du, M.H. Abrahim, M.R. Nordin, Novel modified ZSM-5 as an efficient adsorbent for methylene blue removal, J. Environ. Chem. Eng. 4 (2016) 2607–2616.

[37] S. Rangabhashiyam, N. Anu, M.G. Nandagopal, N. Selvaraju, Relevance of isotherm models in biosorption of pollutants by agricultural byproducts, J. Environ. Chem. Eng. 2 (2014) 398–414.

[38] I. Langmuir, The adsorption of gases on plane surfaces of glass, mica and platinum, J. Am. Chem. Soc. 40 (1918) 1361–1403.

[39] S. Rangabhashiyam, N. Selvaraju, Efficacy of unmodified and chemically modified Swietenia mahagoni shells for the removal of hexavalent chromium from simulated wastewater, J. Mol. Liq. 209 (2015) 487–497.

[40] S. Rangabhashiyam, N. Selvaraju, Evaluation of the biosorption potential of a novel Caryota urens inflorescence waste biomass for the removal of hexavalent chromium from aqueous solutions, J. Taiwan. Inst. Chem. Eng. 47 (2015) 59–70.

[41] S. Rangabhashiyam, N. Selvaraju, Adsorptive remediation of hexavalent chromium from synthetic wastewater by a natural and ZnCl 2 activated Sterculia guttata shell, J. Mol. Liq. 207 (2015) 39–49.

[42] S. Rangabhashiyam, E. Nakkeeran, N. Anu, N. Selvaraju, Biosorption potential of a novel powder prepared from Ficus auriculata leaves, for sequestration of hexavalent chromium from aqueous solutions, Res. Chem. Intermed. 41 (2015) 8405–8424.

[43] H. Freundlich, Uber die adsorption in losungen, Z. Phys. Chem. 57 (1985) 387–470.

[44] M.M. Dubinin, L.V. Radushkevich, Equation of the characteristic curve of activated charcoal, Chem. Zentr. 1 (1947) 875–890.

[45] E. Suganya, S. Rangabhashiyam, A.V. Lity, N. Selvaraju, Removal of hexavalent chromium from aqueous solution by a novel biosorbent Caryota urens seeds: equilibrium and kinetic studies, Desalin. Water Treat. 57 (2016) 23940–23950.

[46] L. Hu, Z. Yang, L. Cui, Y. Li, H.H. Ngo, Y. Wang, Q. Wei, H. Ma, L. Yan, B. Du, Fabrication of hyperbranched polyamine functionalized graphene for high-efficiency removal of Pb (II) and methylene blue, Chem. Eng. J. 287 (2016) 545–556.

[47] S. Rangabhashiyam, N. Selvaraju, B. Raj Mohan, P.K. Muhammed Anzil, K.D. Amith, E.R. Ushakumary, Hydrous cerium oxide nanoparticles impregnated enteromorpha sp. for the removal of hexavalent chromium from aqueous solutions, J. Environ. Sci. Eng. 142 (2015) C4015016.

[48] E. Nakkeeran, S. Rangabhashiyam, M.G. Nandagopal, N. Selvaraju, Removal of Cr (VI) from aqueous solution using Strychnos nux-vomica shell as an adsorbent, Desalin. Water Treat. 57 (2016) 23951–23964.

[49] P. Waranusantigul, P. Pokethitiyook, M. Kruatrachue, E.S. Upatham, Kinetics of basic dye (Methylene Blue) biosorption by giant duckweed (Spirodela polyrrhiza), Environ. Pollut. 125 (2003) 385–392.

[50] J.X. Yu, B.H. Li, X.M. Sun, J. Yuan, R.A. Chi, Polymer modified biomass of baker's yeast for enhancement adsorption of methylene blue, rhodamine B and basic magenta, J. Hazard. Mater. 168 (2009) 1147–1154.

[51] J.X. Yu, B.H. Li, X.M. Sun, J. Yuan, R.A. Chi, Poly(amic acid)-modified biomass of baker's yeast for enhancement adsorption of methylene blue and basic magenta, Appl. Biochem. Biotechnol. 160 (2010) 1394–1406.

[52] Y. Nacera, B. Aicha, Equilibrium and kinetic modelling of methylene blue biosorption by pretreated dead Streptomyces rimosus: effect of temperature, Chem. Eng. J. 119 (2006) 121–125.

[53] Y. Fu, T. Viraraghavan, Removal of a dye from an aqueous solution by the fungus Aspergillus niger, Water Qual. Res. J. Can. 35 (2000) 95–111.

[54] M.C. Ncibi, B. Mahjoub, M. Seffen, Kinetic and equilibrium studies of methylene blue biosorption by Posidonia oceanica (L.) fibres, J. Hazard. Mater. 139 (2007) 280–285.

[55] S. Cengiz, L. Cavas, Removal of methylene blue by invasive marine seaweed: Caulerpa racemosa var. cylindracea, Bioresour. Technol. 99 (2008) 2357–2363.